

Laminated bilayer MoS₂ with weak interlayer coupling

Wenda Zhou¹, Cailei Yuan^{1*}, Aijun Hong¹, Xingfang Luo^{1*}, Wen Lei²

¹Jiangxi Key Laboratory of Nanomaterials and Sensors, School of Physics,
Communication and Electronics, Jiangxi Normal University, 99 Ziyang Avenue,
Nanchang 330022, Jiangxi, China

²School of Electrical, Electronic and Computer Engineering, The University of
Western Australia, 35 Stirling Highway, Crawley 6009, Australia

* Corresponding author. E-mail address: clyuan@jxnu.edu.cn; xfluo@jxnu.edu.cn

Electronic Supplementary Information:

S1: Synthesis diagram of MoS₂ flakes

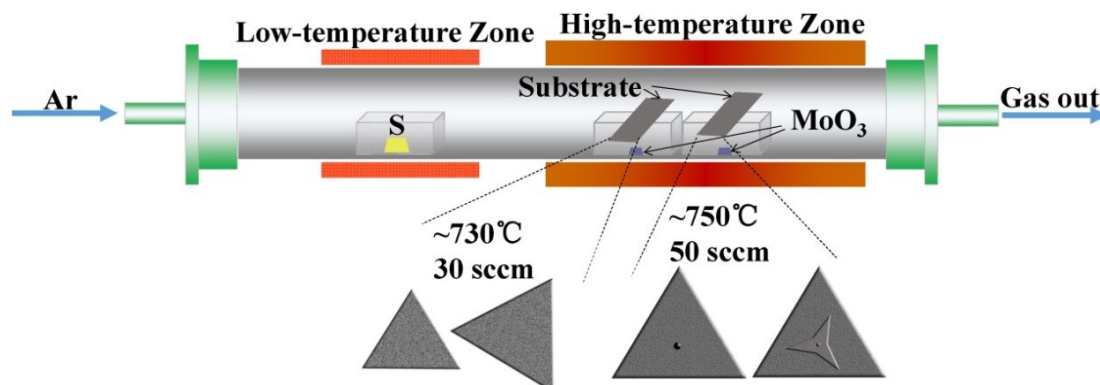


Figure S1 Synthesis diagram of references and test samples with MoS₂ flakes.

S2: XPS analysis of the laminated bilayer MoS₂ flakes

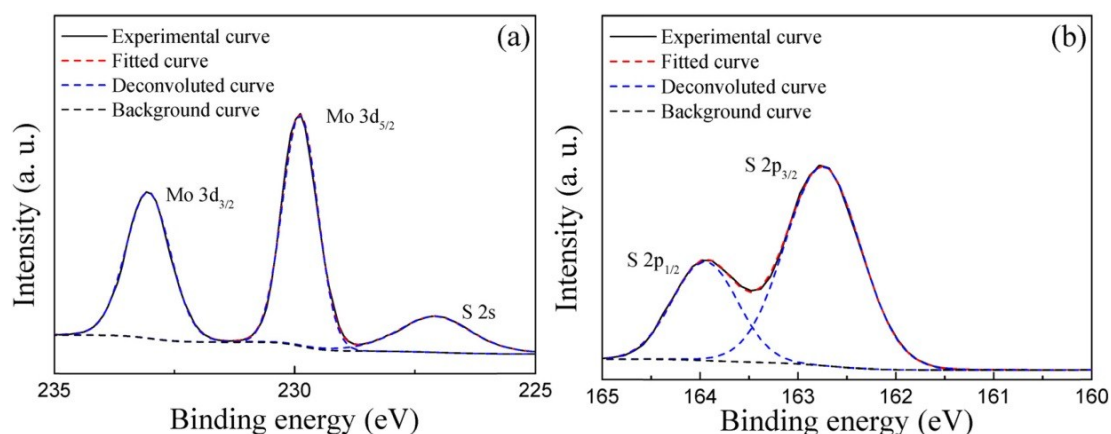


Figure S2 XPS spectra of (a) Mo 3d and (b) S 2p for the laminated bilayer MoS₂ flakes.

The laminated bilayer MoS₂ flakes were characterized with XPS in order to verify its chemical composition. The XPS measurements were carried out with a Kratos XSAM800 spectrometer employing Al K α radiation. The binding energies were corrected for specimen charging by referencing to the C1s peak visible at 285 eV. Figures S2 (a) and (b)

shows the XPS spectra of Mo 3d and S 2p for the laminated bilayer MoS₂ structures as well as their deconvoluted spectra. The Mo 3d XPS spectrum of MoS₂ flakes shows two strong peaks at 233.1 and 229.8 eV, respectively, which are attributed to the doublet Mo 3d_{5/2} and Mo 3d_{3/2}, while the peak at 227.3 eV can be indexed as S 2s. The peaks, corresponding to the S 2p_{1/2} and S 2p_{3/2} orbital of divalent sulfide ions (S²⁻), are observed at 163.9 and 162.8 eV. All these results are well consistent with the corresponding values for the MoS₂ crystal reported previously^{1,2}. Therefore, it can be confirmed that there is no other new phase introduced into the MoS₂ flakes.

S3: AFM and HRTEM analysis of the laminated bilayer MoS₂ with tailored interlayer separation.

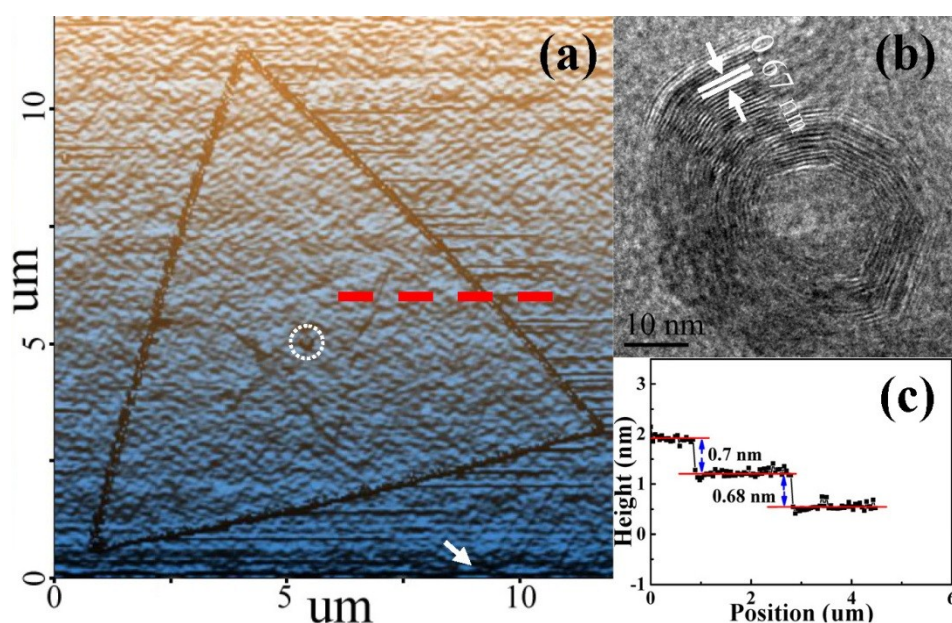


Figure S3 (a) Enhanced color AFM image of a laminated bilayer MoS₂ flake in Sample E; (b) a typical HRTEM image taken from the region encircled in (a); (c) AFM height profiles of a MoS₂ flake along the red dashed line marked in the AFM image (a).

The tunability of interlayer distance was achieved by tuning the size of the MoS₂

nanoparticle between the top and the bottom MoS₂ monolayer, which was realized in experiments by controlling the distance between the SiO₂/Si substrate and the MoO₃ powders during the CVD growth process. To achieve a smaller interlayer distance in comparison to that in sample D, Sample E was prepared by increasing the distance between the SiO₂/Si substrate and the MoO₃ powders from 2.4 cm for Sample D to 2.8 cm for Sample E during the CVD growth process, while keeping other growth conditions the same as those of Sample D. Figure S3 (a) shows the AFM image of Sample E. Similar to Sample D, a three-point star MoS₂ layer is formed on the top of the triangular MoS₂ layer. Figure S3 (b) presents a typical HRTEM image taken from the region encircled in Figure S3 (a). Obviously, a MoS₂ nanoparticle presenting well-stacked layered structure is formed. It should be noted that, the size of the MoS₂ nanoparticle is about 40 nm, which is smaller than that (~60 nm) of the MoS₂ nanoparticle in Sample D. The MoS₂ nanoparticle experiences a size change with the variation of the distance between the precursor and the growth location. This may relate to the concentration gradient of the gas phase MoO₃ along the gas flow direction, which impacts the average growing rate of the MoS₂ crystals. The smaller sized MoS₂ nanoparticle can lead to a smaller interlayer distance for the bilayer MoS₂ structures in Sample E in comparison with Sample D. As shown by the AFM height profile in Figure 6 (c), the interlayer distance in sample E is 0.7 nm, which is less than that (~ 0.72 nm) in Sample D.

S4: PL and Raman spectra analysis of the laminated bilayer MoS₂

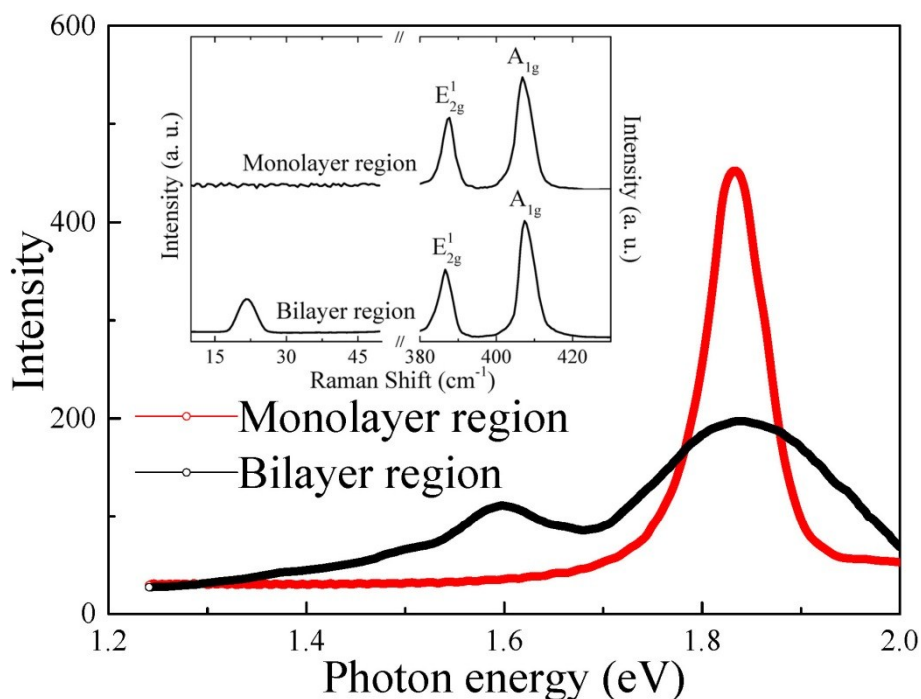


Figure S4 Raman and PL spectra of the laminated bilayer MoS₂ flake in sample E.

In order to understand the physical properties of bilayer MoS₂ structures with different interlayer distance, Raman and PL spectra were undertaken on Sample E, the results of which are shown in Figure S4. As shown by the Raman spectra in the inset of Figure S4, the frequency difference between E_{2g}^1 and A_{1g} Raman modes of bilayer region in Sample E is 20.8 cm⁻¹, which is larger than that of bilayer region in Sample D, while smaller than that of reference bilayer in Sample B. Also, a relatively weaker shear mode signal is also observed for the bilayer region of Sample E in the low frequency range in comparison to the none shear mode signal for the bilayer region in Sample D and the strong shear mode signal for the reference bilayer in Sample B. These results indicate the coupling or van der Waals forces between the adjacent MoS₂ layers for the bilayer MoS₂ structures in Sample E is weaker than that in Sample B, but stronger than that in Sample D, which is caused by the fact that the interlayer distance for the bilayer MoS₂ structures in Sample E is larger than that in

Sample B, but smaller than that in Sample D. As the interlayer coupling conditions have direct impact on the physical properties of the bilayer structures, it provides an effective approach to engineer the physical properties of the bilayer MoS₂ structures. As shown in Figure S4, the PL emission from the bilayer MoS₂ region in sample E presents two PL bands respectively centered at about 1.84 and 1.6 eV. However, it should be noted that the intensity of the PL peak at about 1.84 eV is stronger than that of PL peak at about 1.64 eV. Compared with the PL emission from the bilayer MoS₂ structure in samples B and D, the PL emission from the bilayer MoS₂ structure in Sample E indicates that bandgap structure of laminated bilayer MoS₂ can be well engineered by controlling the interlayer distance and thus interlayer coupling. In addition, a blue-shift (about 4 meV) and a larger FWHM are also observed for the PL peak from bilayer region in Sample E, which is consistent with the PL emission from laminated bilayer MoS₂ in Sample D. These results demonstrate the physical properties of bilayer MoS₂ structures, including energy band structures can be well engineered by controlling the interlayer distance and thus interlayer coupling, which, in experiments can be realized by tuning the size of the MoS₂ nanoparticle via changing the distance between the SiO₂/Si substrate and the MoO₃ powders during the CVD growth process.

References

- (1) Lee, Y. H.; Zhang, X. Q.; Zhang, W.; Chang, M. T.; Lin, C. T.; Chang, K. D.; Yu, Y. C.; Wang, J. T.; Chang, C. S.; Li, L. J.; Lin, T. W. Synthesis of large-area MoS₂ atomic layers with chemical vapor deposition. *Adv. Mater.*, 2012, 24, 2320-2325.
- (2) Fang, H; Tosun, M; Seol, G.; Chang, T. C.; Takei, K.; Guo, J.; Javey, A.

Degenerate n-doping of few-layer transition metal dichalcogenides by potassium. *Nano Lett.* 2013, 13, 1991-1995.